Routledge
Taylor & Francis Group

Connectivity Inference between Neural Structures via Partial Directed Coherence

DANIEL YASUMASA TAKAHASHI*,†, LUIZ ANTONIO BACCALÁ**
& KOICHI SAMESHIMA†,‡

*Bioinformatics Graduate Program, University of São Paulo, Brazil, †Department of Radiology, School of Medicine, University of São Paulo, Brazil, ‡International Institute of Neurosciences of Natal - Edmond and Lily Safra, **Department of Telecommunications and Control Engineering, Escola Politécnica, University of São Paulo, Brazil*

ABSTRACT *This paper describes the rigorous asymptotic distributions of the recently introduced partial directed coherence (PDC) – a frequency domain description of Granger causality between multivariate time series represented by vector autoregressive models. We show that, when not zero, PDC is asymptotically normally distributed and therefore provides means of comparing different strengths of connection between observed time series. Zero PDC indicates an absence of a direct connection between time series, and its otherwise asymptotically normal behavior degenerates into that of a mixture of χ_1^2 variables allowing the computation of rigorous thresholds for connectivity tests using either numerical integration or approximate numerical methods. A Monte Carlo study illustrates the power of the test under PDC nullity. An analysis of electroencephalographic data, before and during an epileptic seizure episode, is used to portray the usefulness of the test in a real application.*

KEY WORDS: Partial directed coherence, epilepsy, Granger causality, connectivity

Introduction

In its quest to understand Nature and its workings, one of Science's core goals is to establish the 'cause and effect' relationship between observations. Controlled experiments are the ideal tools when some variables are accessible. In many cases, however, either because of cost or lack of knowledge as to how to intervene, the underlying implication of events must be deduced from observation alone.

In his 1969 paper, Clive Granger (1969) suggested a concept, now bearing his name, which was influenced by Wiener's general theory of least mean squared error prediction (Wiener, 1956), whereby the evolution of a sequence of time observations (time series) $x_1(k)$ could be seen as *caused* by another observed time sequence $x_2(k)$ if one's ability to predict $x_1(k)$ could be improved significantly by including knowledge of $x_2(k)$'s past as prior available information.

Most practical means of applying these ideas have been focused on time domain approaches by fitting time series prediction models (namely vector autoregressive models) so that hypothesis testing of the nullity of model parameters describing the mutual influence between the time series could be used for inference. In the context of pairs of time series, this idea may quite generally be formalized as:

$$\sigma^2(x_2(k)|x_2(k_-), x_1(k_-)) < \sigma^2(x_2(k)|x_2(k_-)) \tag{1}$$

where $\sigma^2(x_2(k)|\cdot)$ stands for mean squared prediction errors of $x_2(k)$ under, respectively, the conditions of knowledge of the past of $x_2(k)$, denoted by $x_2(k_-)$, or the joint knowledge of both $x_2(k_-)$ and $x_1(k_-)$–the past of $x_1(k)$.

The outstanding property of inequality (1) is that a decrease in prediction error need not hold when $x_1(k)$ and $x_2(k)$ switch positions, i.e. Granger causality is not reciprocal. If $x_1(k)$ Granger causes $x_2(k)$ then it does not necessarily follow that $x_2(k)$ Granger causes $x_1(k)$. Or equivalently the distinctive fact about Granger causality is its unreciprocal nature, i.e.

$$x_1(k) \xrightarrow{Granger} x_2(k) \tag{2}$$

does not imply

$$x_2(k) \xrightarrow{Granger} x_1(k) \tag{3}$$

which means that it allows determining the direction of information flow between observed time sequences. Furthermore, as argued by Sims (1972, failure of either equation (2) or equation (3) furnishes a means for detecting feedback absence. One should additionally note that the present form of causality needs to be properly qualified. In fact, the conclusion that the evolution of a time series is controlling that of another time series is not always justified as discussed by Granger himself (Granger, 1980). An example of this is represented by an unobserved time series that acts upon those under scrutiny, leading to pitfalls of interpretation (Lütkepohl, 1982; Triacca, 1998).

In practice, a simple first-order approximation to detecting the validity of Granger causality is through a linear time series model:

$$x_2(k) = a_{22}(1)x_2(k-1) + a_{22}(2)x_2(k-2) + \ldots$$
$$+ a_{21}(0)x_1(k) + a_{21}(1)x_1(k-1) + \ldots$$

among observed time samples, whereby Granger causality from $x_1(k)$ to $x_2(k)$ holds if one can show that some $a_{21}(r), (r = 1, 2, \ldots)$, significantly differ from zero in a statistical sense. If, in addition, $a_{21}(0)$ is significantly different from zero, one also speaks of instantaneous Granger causality, which is a reciprocal relation unlike Granger causality.

Also, among these time domain approaches one may mention the contributions of Caines & Chan (1975) and Geweke (1982) aimed at comparing pairs of time series. Geweke (1984) considered multivariate time series generalizations as well. Recent practical approaches are described by Lütkepohl (1993) in the multivariate case.

In some areas of science, like neuroscience for example, frequency domain descriptions of many phenomena are of the essence (Daly & Timothy, 1990). In electroencephalography (EEG) for instance, brain states are characterized by well known rhythms ($\alpha, \beta, \ldots$) that have well established clinical and physiological interpretations (Başar, 1998). From the idea that an autoregressive model furnishes a parametric means of spectral description (Priestley, 1981; Marple, 1987) by representing time series spectra as a result of passing the white noise represented by model residuals through filters described by the coefficients

101 of the model, Saito & Harashima (1981) (this was, in fact, preceded by a little-noticed suggestion by Akaike, 1968) proposed a method for gauging Granger causality by factoring the cross-spectral density matrix of bivariate processes by fitting bivariate autoregressive models (see also Schnider *et al.*, 1989). Frequency domain generalizations from the bivariate case soon followed (Kaminski & Blinowska, 1991; Baccalá *et al.*, 1998) and more recently

106 (Baccalá & Sameshima, 2001a). In fact, it was possible to show that these suggestions refer to multivariate time series model factorizations of the cross-spectral matrix associated respectively with ordinary and partial coherence matrices leading respectively to the notions of *directed coherence* (DC) (Baccalá *et al.*, 1998) and *partial directed coherence* (PDC) (Baccalá & Sameshima, 2001c). It is important to mention that the measure proposed in

111 Kaminski & Blinowska (1991) named *direct transfer function* (DTF) differs from DC in how it is normalized. Recent comparative reviews of the properties between DTF and PDC and how they are interpreted can be found in Baccalá & Sameshima (2001b) and Kus *et al.* (2004).

Finally, because these ideas represent a clear approach to the problem of neural

116 connectivity, i.e. that of establishing what neural pathways are active under given situations of behavioral interest, the recent literature in neuroscience has seen many attempts at their systematic use (Fanselow *et al.*, 2001; Korzeniewska *et al.*, 2003).

One serious limitation of studies using the former generalized quantities in neuroscience has, however, thus far been the fact that the criteria used to decide upon the connectivity

121 between observations have largely been obtained through numerical simulations (Schnider *et al.*, 1989; Baccalá & Sameshima, 2001b) that led to essentially arbitrarily imposed thresholds (Sameshima & Baccalá, 1999). The aim of the present paper is to overcome this limitation by providing rigorous asymptotic results on PDC values under mild conditions.

The paper is organized as follows: the partial directed coherence definition is reviewed

126 in the next section together with a statement of the inferential problem. The associated asymptotic results are then stated and are followed by numerical illustrations for both simulated and actual data. The paper ends with a discussion that is followed by the rigorous proofs of its results in the Appendices.

131 ## Background

Given a set $\mathcal{S} = \{x_n(k), 1 \leq n \leq N\}$ of simultaneously observed jointly second-order stationary time series that are described by the pth order vector autoregressive (VAR(p)) model

136
$$
\begin{bmatrix} x_1(k) \\ \vdots \\ x_N(k) \end{bmatrix} = \sum_{r=1}^{p} \mathbf{A}_r \begin{bmatrix} x_1(k-r) \\ \vdots \\ x_N(k-r) \end{bmatrix} + \begin{bmatrix} w_1(k) \\ \vdots \\ w_N(k) \end{bmatrix} \tag{4}
$$

141 where the i, jth entry $a_{ij}(r)$ of the coefficients matrix $\mathbf{A}_r$ describes the linear relationship between time series $x_i(k)$ and $x_j(k)$ at the rth past lag, and $w_i(k)$ represent the driving innovations. For VAR(p) models, testing for the existence of Granger causality from $x_j(k)$ to $x_i(k)$ is equivalent to assessing (Lütkepohl, 1993, p. 39):

146
$$
H : a_{ij}(r) = 0, \quad \forall r \in \{1, \ldots, p\}
$$

The possibility of directly writing the partial coherence between $x_i(k)$ and $x_j(k)$ from the parameters in model (4), i.e. by isolating the interactions between the latter series from those due to the other remaining ones in $\mathcal{S}$ led immediately to the definition of PDC

(Sameshima & Baccalá, 1999; Baccalá & Sameshima, 2001a) as

$$\pi_{ij}(\lambda) = \frac{\bar{A}_{ij}(\lambda)}{\sqrt{\sum_{n=1}^{N} \bar{A}_{nj}(\lambda)\bar{A}_{nj}^{*}(\lambda)}} \quad (5)$$

where

$$\bar{A}_{ij}(\lambda) = \begin{cases} 1 - \displaystyle\sum_{r=1}^{p} a_{ij}(r)\exp(-\mathbf{j}2\pi\lambda r), & if \ i = j \\ -\displaystyle\sum_{r=1}^{p} a_{ij}(r)\exp(-\mathbf{j}2\pi\lambda r), & otherwise \end{cases} \quad (6)$$

with $\mathbf{j} = \sqrt{-1}$ in the exponentials.

Thus, by virtue of equation (6), equation (5) can be considered a frequency domain representation of Granger causality since H holds if and only if $\pi_{ij}(\lambda) \equiv 0$ for all sampling rate normalized frequencies $\lambda \in [-0.5, 0.5]$.

Here we address two related asymptotic problems: the first refers to when

$$H_0 : |\pi_{ij}(\lambda)|^2 = 0$$

is true; whereas the second problem allows finding asymptotic confidence intervals for $|\pi_{ij}(\lambda)|^2$ when H_0 does not hold. This is necessary because distinct limit distributions apply to each case.

To state the final results compactly, it is convenient to introduce the following notation:

$$\bar{\alpha}(\lambda) = vec(\mathbf{I}) - \sum_{r=1}^{p} vec(\mathbf{A}_r)\exp(-\mathbf{j}2\pi\lambda r) \quad (7)$$

where $\mathbf{I}$ is an $N \times N$ identity matrix and vec stands for the usual matrix column stacking operator. Also let

$$\mathbf{a}(\lambda) = \begin{bmatrix} Re(\bar{\alpha}(\lambda)) \\ Im(\bar{\alpha}(\lambda)) \end{bmatrix} \quad (8)$$

This allows rewriting $|\pi_{ij}(\lambda)|^2$ as a ratio of quadratic forms of real normal variables (Lemma 1 in Appendix A)

$$|\pi_{ij}(\lambda)|^2 = \frac{\mathbf{a}^T(\lambda)\mathbf{I}_{ij}^c\mathbf{a}(\lambda)}{\mathbf{a}^T(\lambda)\mathbf{I}_j^c\mathbf{a}(\lambda)} \quad (9)$$

with the matrix

$$\mathbf{I}_{ij}^c = \begin{bmatrix} \mathbf{I}_{ij} & 0 \\ 0 & \mathbf{I}_{ij} \end{bmatrix}$$

where the $N^2 \times N^2$ matrix $\mathbf{I}_{ij}$ is made by zeros except for the entry $(l, m) = ((j-1)N + i, (j-1)N + i)$, which equals 1.

Likewise

$$\mathbf{I}_j^c = \begin{bmatrix} \mathbf{I}_j & 0 \\ 0 & \mathbf{I}_j \end{bmatrix}$$

contains $N^2 \times N^2$ blocks $\mathbf{I}_j$ with zeros except for $(l, m) : (j-1)N + 1 \le l = m \le jN$.

Also let $\bar{\mathbf{\Omega}}$ be the autocovariance of $\hat{\mathbf{a}}$ given by Lemma 2 in Appendix A. Model estimates are based on time series comprising n_s time observations.

Results

PROPOSITION 1 *For a stable stationary Gaussian VAR(p) process, the maximum likelihood estimator $|\hat{\pi}_{ij}(\lambda)|^2$ is* (i) *consistent and* (ii) *asymptotically normal if $|\pi_{ij}(\lambda)|^2 \neq 0$, i.e.,*

$$\sqrt{n_s}\gamma^{-1}(\hat{\mathbf{a}})(|\hat{\pi}_{ij}(\lambda)|^2 - |\pi_{ij}(\lambda)|^2) \xrightarrow{d} \mathcal{N}(0, 1) \tag{10}$$

where

$$\gamma^2(\hat{\mathbf{a}}) = \mathbf{G}(\hat{\mathbf{a}})^T \hat{\bar{\mathbf{\Omega}}} \mathbf{G}(\hat{\mathbf{a}})$$

and

$$\mathbf{G}(\hat{\mathbf{a}}) = 2(\mathbf{I}_{ij}^c \hat{\mathbf{a}})(\hat{\mathbf{a}}^T \mathbf{I}_j^c \hat{\mathbf{a}})^{-1} - 2(\mathbf{I}_j^c \hat{\mathbf{a}})(\hat{\mathbf{a}}^T \mathbf{I}_j^c \hat{\mathbf{a}})^{-2}(\hat{\mathbf{a}}^T \mathbf{I}_{ij}^c \hat{\mathbf{a}})$$

In these equations $\mathbf{a}$'s dependence on λ was omitted. This is done throughout the text when no danger of confusion exists.

Since $G(\mathbf{a}) = 0$ when H_0 holds, the first-order approximation result in equation (10) fails and calculation of higher order terms in the expansion of $|\hat{\pi}_{ij}(\lambda)|^2$ becomes necessary. This leads to Proposition 2.

PROPOSITION 2 *When H_0 holds, under the conditions of Proposition 1,*

$$n_s(\hat{\mathbf{a}}^T \mathbf{I}_i^c \hat{\mathbf{a}})(|\hat{\pi}_{ij}(\lambda)|^2 - |\pi_{ij}(\lambda)|^2) \xrightarrow{d} \sum_{k=1}^{q} l_k \chi_1^2 \tag{11}$$

where l_k are the eigenvalues of $\mathbf{D} = \mathbf{L}^T \mathbf{I}_{ij}^c \mathbf{L}$, in which the matrix $\mathbf{L}$ is the Choleski factor in

$$\bar{\mathbf{\Omega}} = \mathbf{L}\mathbf{L}^T$$

with $q = rank(\mathbf{D}) = 2$, unless $\lambda \in \{0, \pm 0.5\}$ or $p = 1$ when $q = 1$.

Computation of quantile thresholds in equation (11) calls either for the use of numerical methods or the employment of approximate computations (Appendix B). Practical hypothesis testing may proceed on a λ value basis.

Numerical Illustrations

Simulated Data

To assess the practical validity of the present results we performed Monte Carlo simulations using 10,000 replications for $n_s = 100, 500, 1000$, and 10,000 observed data points of the following VAR(2) model:

$$\begin{bmatrix} x_1(n) \\ x_2(n) \\ x_3(n) \end{bmatrix} = \begin{bmatrix} 0.2 & -0.4 & 0.3 \\ a_{21}(1) & 0.8 & 0.4 \\ 0 & -0.1 & 0.4 \end{bmatrix} \begin{bmatrix} x_1(n-1) \\ x_2(n-1) \\ x_3(n-1) \end{bmatrix}$$
$$+ \begin{bmatrix} 0 & -0.2 & 0 \\ 0 & -0.1 & 0 \\ 0.5 & 0.2 & 0.1 \end{bmatrix} \begin{bmatrix} x_1(n-2) \\ x_2(n-2) \\ x_3(n-2) \end{bmatrix} + \begin{bmatrix} w_1(n) \\ w_2(n) \\ w_3(n) \end{bmatrix} \tag{12}$$

where $w_i(n)$ are mutually uncorrelated standard Gaussian innovations.
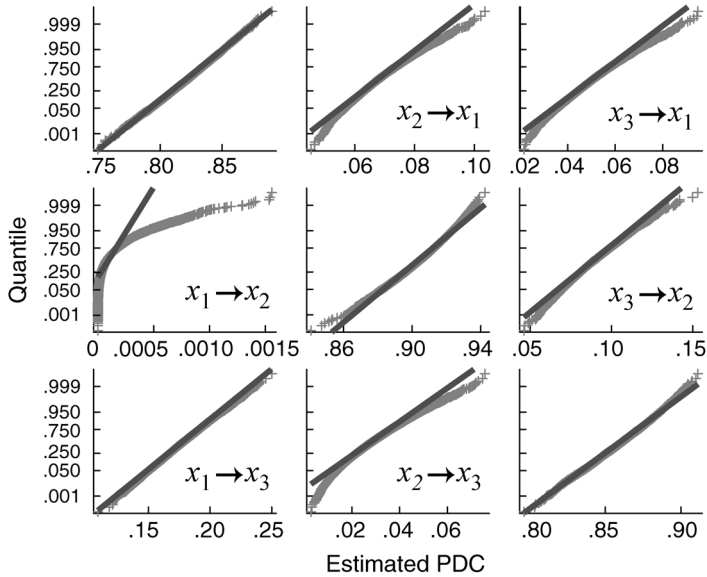
Figure 1. Normal plots for PDC estimates for each pair of observed time series for $n_s = 1000$. Note the deviation from normality under H_0 when evaluating $x_1 \rightarrow x_2$. The computations refer to $\lambda = 0.3$. Note also that, when PDC values are closer to the extremes (toward 0 and 1), the normal approximation degrades accordingly. Panels along the main diagonal represent the normal plots of $|\pi_{ii}(0.3)|^2$ for $i = 1, 2,$ and 3

An illustration of the PDC distribution pattern for $a_{21}(1) = 0$ and $\lambda = 0.3$ is provided by the normal plots in Figure 1, where normality is evident except for the relationship from $x_1(n)$ to $x_2(n)$ in which Granger causality is absent. Observe that tail deviation increases for PDC values close to the extremes 0 and 1. A more detailed distribution adjustment picture, when H_0 holds, is presented in Figure 2 by contrasting equation (11) to both the empirical distribution obtained via Monte Carlo simulations (10 000 realizations) and the distribution of a $c\chi_v^2$ random variable, where $c = \sum_{k=1}^{q} l_k^2 / \sum_{k=1}^{q} l_k$ and $v = \left(\sum_{k=1}^{q} l_k \right)^2 / \sum_{k=1}^{q} l_k^2$
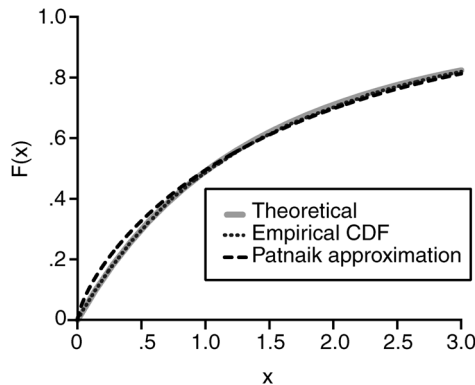
Figure 2. Theoretical (in solid gray), empirical (in dotted black), and Patnaik approximated $c\chi_v^2$ (in dashed black) cumulative density functions for $n_s = 1000$ under the null hypothesis (i.e. $|\pi_{21}(0.3)|^2 = 0$) for the simulated model in equation (12). The x-axis corresponds to the left-hand side of equation (11)

301

Table 1. Percentile points for the empirical, theoretical and Patnaik approximate cumulative distributions for $n_s = 1000$ under the null hypothesis (i.e. $|\pi_{21}(0.3)|^2 = 0$) for the simulated model in equation (12)

Cumulative distribution	Percentile point			
	1%	5%	10%	15%
Empirical	0.014	0.071	0.146	0.230
Theoretical	0.013	0.069	0.143	0.222
Patnaik	0.003	0.031	0.085	0.153

306

311

(the Patnaik approximation, cf. Appendix B). These parameters were obtained adjusting the first- and second-order moments of the right-hand side of equation (11) and $c\chi_v^2$. A Kolmogorov–Smirnov test did not reject the null hypothesis of equality of the empirical and theoretical distributions, at 5%, and showed that the estimated PDC distribution conforms to the theoretical asymptotic distribution in equation (11). Table 1 shows a comparison of the 1, 5, 10 and 15 percentile points of the cumulative distributions in the empirical, theoretical and Patnaik approximation cases. In this example, one can see that the empirical and theoretical percentile values closely match while for the Patnaik approximation they were underestimated.

316

In fact, the use of Proposition 2 leads to observed percentage rates of rejecting H_0 of 5.86, 5.22, 5.12, and 4.71, respectively, for $n_s = 100, 500, 1000$, and $10\,000$ time series points. The test powers for different values of PDC, gauged by Monte Carlo simulations (10,000 realizations), are contrasted in Tables 2 and 3, respectively, for thresholds obtained by direct computation of probability function in equation (B.1) and by the Patnaik approximation (see Appendix B for more details).

321

326

Neurobiological Example. Three time series (T3, T4, and O1), selected from standard international 10-20 EEG system, sampled at 200 Hz and derived from a patient with left mesial temporal lobe epilepsy, with seizure focus roughly localized at the T3 channel area, clinically diagnosed and post-surgically confirmed at the Neurological Division of Hospital das Clínicas from the University of São Paulo, are used for the present illustration. Two distinct data segments (each with 1000 data points, i.e. 5 s), during and immediately before a seizure onset, separated by 20 s to exclude the transition period, were used in characterizing the relationship between brain areas. The present choices were motivated by their importance toward understanding the physiopathological basis of epilepsy and the immediate

331

336

Table 2. Power of the proposed test for model given by equation (12) for different $a_{21}(1)$ values under the nominal significance level of 5%, at $\lambda = 0.3$, using quantiles given by Theorem 2

341

$a_{21}(1)$	$|\pi_{21}(0.3)|^2$	Percentage of rejection (%)			
		$n_s = 100$	$n_s = 500$	$n_s = 1000$	$n_s = 10\,000$
0	0	5.86	5.22	5.12	4.71
0.05	0.0018	7.33	14.16	24.77	99.51
0.10	0.0070	13.93	45.73	78.10	100
0.15	0.0157	23.69	82.84	99.10	100
0.20	0.0275	38.43	98.05	99.99	100
0.50	0.1503	99.33	100	100	100

346

Table 3. Power of the proposed test for model given by equation (12) under the nominal significance level of 5%, at $\lambda = 0.3$, using the Patnaik approximation

$a_{21}(1)$	$\lvert\pi_{21}(0.3)\rvert^2$	Percentage of rejection (%)			
		$n_s = 100$	$n_s = 500$	$n_s = 1000$	$n_s = 10\,000$
0	0	5.64	5.12	5.02	4.77
0.05	0.0018	7.11	13.96	24.49	99.51
0.10	0.0070	13.68	45.38	77.85	100
0.15	0.0157	23.24	82.58	99.09	100
0.20	0.0275	37.83	98.02	99.99	100
0.50	0.1503	99.33	100	100	100

application of the present method to clinical diagnosis support. Further empirical studies of EEG recordings from patients with temporal lobe epilepsy using PDC can be found in Baccalá *et al.* (2004).

Three-variate models were estimated for each segment with model orders obtained via Akaike's information criterion (Lütkepohl, 1993, p. 129) leading to $p = 4$ and $p = 5$, respectively, to each segment. Estimated model adequacy was ensured by a Portmanteau test on the residual autocorrelations whose whiteness could not be rejected at 5% (Lütkepohl, 1993, p. 150).

After PDC computation, null hypothesis tests were performed for each frequency ($\lambda = 1, 2, \ldots, 49$ Hz) and each channel pair at 5%. When H_0 could be rejected, confidence intervals were computed under the normal approximation, leading to Figures 3 and 4. For comparison in these figures, an asterisk indicates rejection of the absence of Granger causality by a standard time domain Wald test at 5% (Lütkepohl, 1993, p. 94).
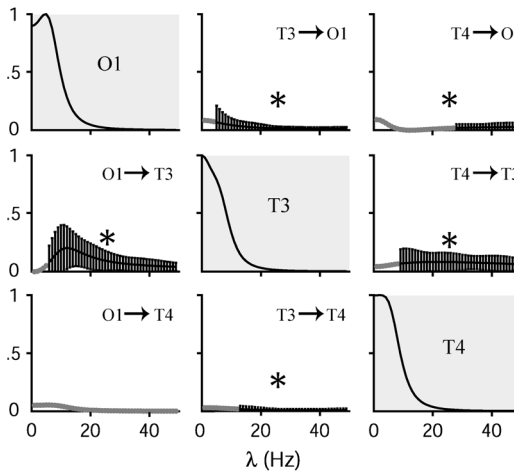
Before seizure onset, there are no significant interactions at frequencies lower than 5 Hz, even though PDC is significant for higher frequencies (Figure 3). On the other hand, during
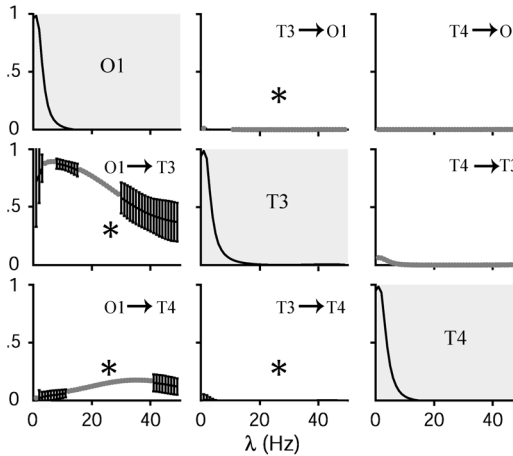

Figure 3. Estimated PDC values between O1, T3, and T4 channels preceding the seizure onset. Normalized power spectrum densities are shown by the panels along the main diagonal. Only values for $1\,\text{Hz} \leq \lambda \leq 49\,\text{Hz}$ were plotted due to the physiological significance. Line segments in gray represent those frequencies in which null hypotheses were not rejected at 5% level, while 95% confidence intervals are provided in black for rejected frequencies at 5%. Channel pairs with significant time domain Granger causality at 5% are indicated by an asterisk

401

406

411

Figure 4. Estimated PDC values between O1, T3, and T4 channels during the seizure. See legend to Figure 3 for further explanation

416

the seizure there are significant interactions between the channels for lower frequencies (Figure 4). This is in accord with physiological data, as temporal lobe seizures are characterized by both low frequency oscillations ($\approx 5\,\text{Hz}$) and channel synchronization (Daly & Timothy, 1990). Also of note is the significant increase of PDC from O1 to T3 during the seizure when compared to the other segment, thereby matching the fact that T3 is the epilepsy-focus brain area (Baccalá *et al.*, 2004).

421

Those channel pairs with significant interactions in the frequency domain (PDC test) were also significant in the time domain (Granger causality test); the converse being true as well.

426

Discussion

Partial directed coherence was proposed as a frequency domain counterpart of the Granger causality concept for VAR models (Baccalá & Sameshima, 2001c). The asymptotic distribution of its maximum likelihood estimator was derived for normally distributed VAR coefficients. This result opens the way for objectively comparing the difference of the strength of connection between time series.

431

Approximate confidence intervals and a test for null PDC was proposed. A Monte Carlo experiment showed the reasonable power attainable by the test under mild sample size ($n_s = 1000$).

436

An alternative derivation of the asymptotic statistics under the null hypothesis has been recently provided by Schelter *et al.* (2006) who furnish additional applied examples. The equivalence of the Schelter *et al.* (2006) results follows from the fact that the non-zero eigenvalues of $\mathbf{D} = \mathbf{L}^T \mathbf{I}_{ij}^c \mathbf{L}$ are the same as those of $\mathbf{I}_{ij}^c \mathbf{L} \mathbf{L}^T \mathbf{I}_{ij}^c$ which has only four non-necessarily zero entries that are responsible for the two eigenvalues of $\mathbf{D}$ that are not necessarily zero (note that $(\mathbf{I}_{ij}^c)^2 = \mathbf{I}_{ij}^c$).

441

Because of its ready interpretability in the frequency domain, especially in neuroscience, the present rigorous hypothesis testing results provide more information than traditional time domain Granger causality tests.

446

The application of PDC analysis to neurobiological data is promising and allows unraveling biologically interesting results. Recent applications of PDC in experimental work can be found elsewhere (Fanselow *et al.*, 2001; Baccalá *et al.*, 2004; Supp *et al.*, 2005).

References

Akaike, H. (1968) On the use of a linear model for the identification of feedback systems, *Annals of the Institute of Statistical Mathematics*, 20(3), pp. 425–439.

Baccalá, L.A. & Sameshima, K. (2001a) Overcoming the limitations of correlation analysis for many simultaneously processed neural structures, *Progress in Brain Research*, 130, pp. 33–47.

Baccalá, L.A. & Sameshima, K. (2001b) Partial directed coherence: A new concept in neural structure determination, *Biological Cybernetics*, 84(6), pp. 463–474.

Baccalá, L.A. & Sameshima, K. (2001c) Partial directed coherence: Some estimation issues, in: F. Rattay (ed.) *World Congress on Neuroinformatics*, pp. 546–553 (Vienna: ARGESIM/ASIM Verlag).

Baccalá, L.A., Sameshima, K., Ballester, G., Valle, A.C. & Timo-Iaria, C. (1998) Studying the interaction between brain structures via directed coherence and Granger causality, *Applied Signal Processing*, 5(1), pp. 40–48.

Baccalá, L.A., Alvarenga, M.Y., Sameshima, K., Jorge, C.L. & Castro, L.H. (2004) Graph theoretical characterization and tracking of the effective neural connectivity during episodes of mesial temporal epileptic seizure, *Journal of Integrative Neuroscience*, 3(4), pp. 379–395.

Başar, E. (1998) *Brain Function and Oscillations: Brain Oscillations. Principles and Approaches* (Berlin: Springer-Verlag).

Caines, P.E. & Chan, C.W. (1975) Feedback between stationary stochastic processes, *IEEE Transactions on Automatic Control*, 20(4), pp. 498–508.

Daly, D.D. & Timothy, A.P. (1990) *Current Practice of Clinical Electroencephalography* (New York: Raven Press).

Fanselow, E.E., Sameshima, K., Baccalá, L.A. & Nicolelis, M. A.L. (2001) Thalamic bursting in rats during different awake behavioral states, *Proceedings of the National Academy of Sciences of the United States of America*, 98(26), pp. 15330–15335.

Farebrother, R.W. (1990) Algorithm as 256: The distribution of a quadratic form in normal variable, *Applied Statistics*, 39(2), pp. 249–309.

Geweke, J. (1982) Measurement of linear dependence and feedback between multiple time series, *Journal of the American Statistical Association*, 77(378), pp. 304–324.

Geweke, J.F. (1984) Measures of conditional linear dependence and feedback between time series, *Journal of the American Statistical Association*, 79(388), pp. 907–915.

Granger, C.W.J. (1969) Investigating causal relations by econometric models and cross-spectral methods, *Econometrica*, 37(3), pp. 424–438.

Granger, C.W.J. (1980) Testing for causality: A personal viewpoint, *Journal of Economic Dynamics and Control*, 2, pp. 329–352.

Imhof, J.P. (1961) Computing the distribution of quadratic forms in normal variables, *Biometrika*, 48(3-4), pp. 419–426.

Johnson, N.L., Kotz, S. & Balakrishnan, N. (1995) *Continuous Univariate Distributions*, vol. 2 (New York: Wiley).

Kaminski, M.J. & Blinowska, K. J. (1991) A new method of the description of the information flow in the brain structures, *Biological Cybernetics*, 65(3), pp. 203–210.

Korzeniewska, A., Manczak, M., Kaminski, M., Blinowska, K.J. & Kasicki, S. (2003) Determination of information flow direction among brain structures by a modified directed transfer function (dDTF) method, *Journal of Neuroscience Methods*, 125(1–2), pp. 195–207.

Kus, R., Kaminski, M. & Blinowska, K. (2004) Determination of EEG activity propagation: Pair-wise versus multichannel estimate, *IEEE Transactions on Biomedical Engineering*, 51(9), pp. 1501–1510.

Lütkepohl, H. (1982) Non-causality due to omitted variables, *Journal of Econometrics*, 19(2-3), pp. 367–378.

Lütkepohl, H. (1993) *Introduction to Multiple Time Series Analysis* (Berlin: Springer-Verlag).

Marple, S.L. Jr (1987) *Digital Spectral Analysis* (New Jersey: Prentice Hall).

Patnaik, P.B. (1949) The non-central χ^2 and F-distributions and their applications, *Biometrika*, 36(1–2), pp. 202–232.

Priestley, M.B. (1981) *Spectral Analysis and Time Series, Two-Volume Set, Volumes I and II* (London: Academic Press).

Saito, Y. & Harashima, H. (1981) Tracking of information within multichannel EEG record - causal analysis in EEG, in: N. Yamaguchi & K. Fujisawa (eds) *Recent Advances in EEG and EMG Data Processing*, pp. 133–146 (Amsterdam: Elsevier).

Sameshima, K. & Baccalá, L.A. (1999) Using partial directed coherence to describe neuronal ensemble interactions, *Journal of Neuroscience Methods*, 94(1), pp. 93–103.

Schelter, B., Winterhalder, M., Eichler, M., Peifer, M., Hellwig, B., Guschlbauer, B. Lucking, C., Dahlhaus, R. & Timmer, J. (2006) Testing for directed influences among neural signals using partial directed coherence, *Journal of Neuroscience Methods*, 152(1–2), pp. 210–219.

Schnider, S.M., Kwong, R.H., Lenz, F.A. & Kwan, H.C. (1989) Detection of feedback in the central nervous system using system identification techniques, *Biological Cybernetics*, 60(3), pp. 203–212.

Serfling, R.J. (1980) *Approximation Theorems of Mathematical Statistics* (New York: Wiley).

Sims, C.A. (1972) Money, income, and causality, *American Economic Review*, 62(4), pp. 540–552.

Supp, G.G., Schlogl, A., Fiebach, C.J., Gunter, T.C., Vigliocco, G., Pfurtscheller, G. & Petsche, H. (2005) Semantic memory retrieval: cortical couplings in object recognition in the n400 window, *European Journal of Neuroscience*, 21(4), pp. 1139–1143.

Triacca, U. (1998) Non-causality: The role of the omitted variables, *Economics Letters*, 60(3), pp. 317–320.

Wiener, N. (1956) The theory of prediction, in: E.F. Beckenbach (ed.) *Modern Mathematics for Engineers*, Series 1, pp. 125–139 (New York: McGraw-Hill).

Appendix A

Let $\alpha = vec[\mathbf{A}_1 \ldots \mathbf{A}_p]$. Consider $N^2 \times pN^2$ dimensional matrices

$$\mathbf{C}(\lambda) = [\mathbf{C}_1(\lambda) \ldots \mathbf{C}_p(\lambda)]$$

and

$$\mathbf{S}(\lambda) = [\mathbf{S}_1(\lambda) \ldots \mathbf{S}_p(\lambda)]$$

such that

$$\mathbf{C}_r(\lambda) = diag([cos(2\pi r\lambda) \ldots cos(2\pi r\lambda)])$$

and

$$\mathbf{S}_r(\lambda) = diag([sin(2\pi r\lambda) \ldots sin(2\pi r\lambda)])$$

Hence equation (7) can be rewritten as

$$\bar{\alpha}(\lambda) = vec(\mathbf{I}) - (\mathbf{C}(\lambda) - \mathbf{j}\mathbf{S}(\lambda))\alpha$$

(for $\mathbf{j} = \sqrt{-1}$) and equation (8) as

$$\mathbf{a}(\lambda) = \begin{bmatrix} vec(\mathbf{I}) \\ \mathbf{0} \end{bmatrix} - \mathcal{C}(\lambda) \begin{bmatrix} \alpha \\ \alpha \end{bmatrix} \tag{A.1}$$

where

$$\mathcal{C}(\lambda) = \begin{bmatrix} \mathbf{C}(\lambda) & \mathbf{0} \\ \mathbf{0} & -\mathbf{S}(\lambda) \end{bmatrix}$$

Then simple substitution produces:

$$\mathbf{a}^T(\lambda)\mathbf{I}_{ij}^c\mathbf{a}(\lambda) = |\bar{A}_{ij}(\lambda)|^2$$

and

$$\mathbf{a}^T(\lambda)\mathbf{I}_j^c\mathbf{a}(\lambda) = \sum_{n=1}^{N} \bar{A}_{nj}(\lambda)\bar{A}_{nj}^*(\lambda)$$

where the roles of $\mathbf{I}_{ij}^c$ and $\mathbf{I}_j^c$ are to select the necessary variables from $\mathbf{a}(\lambda)$ in writing $|\pi_{ij}(\lambda)|^2$. This proves the following Lemma.

551   LEMMA 1   *PDC defined by equation (5) can be written as the ratio of real quadratic forms given by equation (9).*

   To obtain the asymptotic behavior of the estimators of interest, the starting point is the following fundamental lemma.

556

LEMMA 2   *For a stationary stable Gaussian VAR(p) process as defined in model (4), the maximum likelihood estimator of* **a** *is consistent and*

$$\sqrt{n_s}(\hat{\mathbf{a}}(\lambda) - \mathbf{a}(\lambda)) \xrightarrow{d} \mathcal{N}(0, \bar{\boldsymbol{\Omega}}(\lambda))$$

561

where

$$\bar{\boldsymbol{\Omega}}(\lambda) = \mathcal{C}(\lambda)\boldsymbol{\Omega}_a \mathcal{C}(\lambda)^T \tag{A.2}$$

for

566

$$\boldsymbol{\Omega}_a = \begin{bmatrix} \boldsymbol{\Omega} & \boldsymbol{\Omega} \\ \boldsymbol{\Omega} & \boldsymbol{\Omega} \end{bmatrix}$$

Here, $\boldsymbol{\Omega} = \boldsymbol{\Gamma}_{\mathbf{x}}(0)^{-1} \otimes \boldsymbol{\Sigma}_{\mathbf{w}}$ *where* $\boldsymbol{\Gamma}_{\mathbf{x}}(0)$ *and* $\boldsymbol{\Sigma}_{\mathbf{w}}$ *stand, respectively, for autocovariance matrices of the data*

571

$$\mathbf{x} = [x_1(k) \dots x_N(k) \dots x_1(k - p + 1) \dots x_N(k - p + 1)]^T$$

and of the innovations

$$\mathbf{w} = [w_1(k) \dots w_N(k)]^T$$

The operator $\otimes$ *is the Kronecker product.*

576

Proof   The lemma is a direct consequence of the result

$$\sqrt{n_s}(\hat{\boldsymbol{\alpha}} - \boldsymbol{\alpha}) \xrightarrow{d} \mathcal{N}(0, \boldsymbol{\Gamma}_{\mathbf{x}}(0)^{-1} \otimes \boldsymbol{\Sigma}_{\mathbf{w}})$$

581   (see Lütkepohl, 1993, after building **a**(λ) as in equation (A.1), so that straightforward calculation of its covariance leads to equation (A.2).
   This completes the proof.   ∎

Proof of Proposition 1
586   *Proof*
The proof follows directly from the following version of the delta method (Serfling, 1980) for a real differentiable function $g(\mathbf{a}(\lambda))$ $(= |\pi_{ij}(\lambda)|^2)$ of the normal vectors $\mathbf{a}(\lambda)$ (guaranteed by Lemma 2) whereby

591

$$\sqrt{n_s}(g(\hat{\mathbf{a}}) - g(\mathbf{a})) \xrightarrow{d} \mathcal{N}(0, \mathbf{G}^T \boldsymbol{\Sigma} \mathbf{G})$$

where $\mathbf{G} = \nabla_{\mathbf{a}} g$ is the standard vector gradient of g in equation (9) computed at **a**. The proposition is obtained by straightforward computation of **G** recognizing $\boldsymbol{\Sigma} = \bar{\boldsymbol{\Omega}}$ in Lemma 2. Slutsky's lemma allows using estimated quantities in lieu of the actual values completing
596   the proof.   ∎

Proof of Proposition 2
Proof
Consider the following generalized version of the delta method (Serfling, 1980):

601 THEOREM 1 *Suppose $X_n = (X_{n1}, \ldots, X_{nk})^T$ with*

$$\sqrt{n}(X_n - \mu) \xrightarrow{d} \mathcal{N}(0, \Sigma)$$

606 *Let $g(x)$ be a real-valued function with continuous partials of order $m > 1$ in the neighborhood of $x = \mu$, with all the partials of order j with $1 \leq j \leq m - 1$ vanishing at $x = \mu$ and non-vanishing mth order partials at $x = \mu$. Then*

611
$$(\sqrt{n})^m (g(X_n) - g(\mu)) \xrightarrow{d} \frac{1}{m!} \sum_{i_1=1}^{k} \cdots \sum_{i_m=1}^{k} \frac{\partial^m g}{\partial x_{i_1} \ldots \partial x_{i_m}} \Big|_{x=\mu} \prod_{j=1}^{m} Z_{i_j}$$

with

$$Z = (Z_1, \ldots, Z_k)^T \sim \mathcal{N}(0, \Sigma)$$
616

Since the first-order ($m = 1$) partial derivatives of $g(\mathbf{a})$ are zero under H_0 ($\mathbf{G}(\mathbf{a}) = 0$), one may employ the next level of approximation given by Theorem 1. Therefore, computing the second-order ($m = 2$) derivatives of $g(\mathbf{a}(\lambda))$, and noting $g(\mathbf{a}(\lambda)) = 0$ under H_0 implies that $\mathbf{I}_{ij}^c \mathbf{a}(\lambda) = 0$, hence leading to

621
$$\frac{\partial^2 g(\mathbf{a}(\lambda))}{\partial \mathbf{a}(\lambda) \partial \mathbf{a}^T(\lambda)} \Big|_{\mathbf{I}_{ij}^c \mathbf{a}(\lambda)=0} = 2\mathbf{I}_{ij}^c (\mathbf{a}^T(\lambda) \mathbf{I}_j^c \mathbf{a}(\lambda))^{-1}$$

626 or equivalently in equation () **Q1**

$$n_s(\hat{\mathbf{a}}^T(\lambda) \mathbf{I}_j^c \hat{\mathbf{a}}(\lambda))(|\hat{\pi}_{ij}(\lambda)|^2 - |\pi_{ij}(\lambda)|^2) \xrightarrow{d} \mathbf{x}^T \mathbf{I}_{ij}^c \mathbf{x}$$

631 for $\mathbf{x} \xrightarrow{d} \mathcal{N}(0, \bar{\Omega})$, so that the use of Slutsky's lemma concludes the first part of the proof by allowing the use of estimated quantities.

It is possible to compute $\mathbf{x}^T \mathbf{I}_{ij}^c \mathbf{x}$ from conveniently transformed variables. If this transformation is done through the matrix $\mathbf{L}$ obtained from the Choleski decomposition of $\bar{\Omega} = \mathbf{L}\mathbf{L}^T$ one may write $\mathbf{x} = \mathbf{L}\mathbf{y}$, so that $\mathbf{x}^T \mathbf{I}_{ij}^c \mathbf{x} = \mathbf{y}^T \mathbf{L}^T \mathbf{I}_{ij}^c \mathbf{L}\mathbf{y} = \mathbf{y}^T \mathbf{D}\mathbf{y}$. This choice of new trans-
636 formed variables in the vector $\mathbf{y} = (\mathbf{L}^T \mathbf{L})^{-1} \mathbf{L}^T \mathbf{x}$ makes them mutually independent zero mean unit variance, in fact,

$$E[\mathbf{y}\mathbf{y}^T] = (\mathbf{L}^T \mathbf{L})^{-1} \mathbf{L}^T E[\mathbf{x}\mathbf{x}^T] \mathbf{L} (\mathbf{L}^T \mathbf{L})^{-1} = (\mathbf{L}^T \mathbf{L})^{-1} \mathbf{L}^T \mathbf{L}\mathbf{L}^T \mathbf{L} (\mathbf{L}^T \mathbf{L})^{-1} = \mathbf{I}$$
641

Now diagonalizing $\mathbf{D} = \mathbf{L}^T \mathbf{I}_{ij}^c \mathbf{L} = \mathbf{U}\Lambda\mathbf{U}^T$ with $\mathbf{U}\mathbf{U}^T = \mathbf{I}_{q \times q}$ produces

$$\mathbf{y}^T \mathbf{D}\mathbf{y} = \sum_{k=1}^{q} l_k \mathbf{y}^T \mathbf{u}_k \mathbf{u}_k^T \mathbf{y} = \sum_{k=1}^{q} l_k \zeta_k^2$$
646

where $\mathbf{u}_k$ is the kth column of $\mathbf{U}$. It is easy to show that the variables $\zeta_k = \mathbf{u}_k^T \mathbf{y}$ are mutually independent, Gaussian zero mean and of unit variance so that their squares are χ_1^2 random variables.

As $rank(\mathbf{X}) = rank(\mathbf{X}^T)$ and $rank(\mathbf{XY}) \leq \min(rank(\mathbf{X}), rank(\mathbf{Y}))$, it follows that

$$
\begin{aligned}
rank(\mathbf{D}) &= rank(\mathbf{L}^T \mathbf{I}_{ij}^c \mathbf{L}) \\
&= rank(\mathbf{L}^T \mathbf{I}_{ij}^c \mathbf{I}_{ij}^c \mathbf{L}) \\
&= rank(\mathbf{I}_{ij}^c \mathbf{L} \mathbf{L}^T \mathbf{I}_{ij}^c) \\
&= rank(\mathbf{I}_{ij}^c \bar{\mathbf{\Omega}}(\lambda) \mathbf{I}_{ij}^c) \\
&= rank(\mathbf{I}_{ij}^c \mathcal{C}(\lambda) \mathbf{\Omega}_a \mathcal{C}(\lambda)^T \mathbf{I}_{ij}^c)
\end{aligned}
$$

which is upper bounded by $rank(\mathbf{I}_{ij}^c) = 2$. It is readily verified that, when $\lambda \in \{0, \pm 0.5\}$, $rank(\mathcal{C}(\lambda)) = 1$ imposing the upper bound. Also, when $p = 1$, $rank(\mathbf{I}_{ij}^c \mathcal{C}(\lambda) \mathbf{\Omega}_a \mathcal{C}(\lambda)^T \mathbf{I}_{ij}^c) = 1$ regardless of λ because, in this case, the largest non-vanishing minor in the matrix is

$$
\mathbf{\Omega}_{(j-1)N+i}
\begin{bmatrix}
\cos^2(2\pi\lambda) & \sin(2\pi\lambda)\cos(2\pi\lambda) \\
\sin(2\pi\lambda)\cos(2\pi\lambda) & \sin^2(2\pi\lambda)
\end{bmatrix}
$$

whose rank is 1, where $\mathbf{\Omega}_{(j-1)N+i}$ is the $((j-1)N+i, (j-1)N+i)$ entry of $\mathbf{\Omega}$, thereby concluding the proof. ∎

Appendix B. Quantile Computations

The p-value computations in this paper have been made using the following numerical inversion formula of the characteristic function:

THEOREM 2 (Imhof, 1961)

- *The characteristic function of the right-hand side of equation* (11) *is*

$$
\phi(t) = \prod_{k=1}^{K} (1 - 2\mathbf{j}l_k t)^{-1/2}
$$

with $\mathbf{j} = \sqrt{-1}$.
- *The imaginary part of* $\exp(-jux\phi(u))$ *is expressed as* $\sin\theta(u)/\rho(u)$, *where*

$$
\theta(u) = \frac{1}{2} \sum_{k=1}^{K} \{\tan^{-1}(l_k u)\} - \frac{xu}{2}
$$

and

$$
\rho(u) = \prod_{k=1}^{K} (1 + l_k^2 u^2)^{1/4}
$$

- *The function* $u\rho(u)$, $u \geq 0$, *increases monotonically toward* $+\infty$. *Hence, in numerical procedure, the integration in the inversion formula*

$$
\mathbb{P}(\mathbf{y}^T \mathbf{D} \mathbf{y} \leq x) = \frac{1}{2} - \frac{1}{\pi} \int_0^{\infty} \frac{\sin\theta(u)}{u\rho(u)} du \tag{B.1}
$$

may be carried over a finite range $0 \leq u \leq U$ *with error of truncation* t_U, *which satisfies*

$$
|t_U| \leq \left(\pi \frac{K}{2} U^{K/2} \prod_{k=1}^{K} |l_k|^{1/2} \right)^{-1}
$$

701 • *The probability density function can be obtained by*

$$p(x) = \frac{1}{\pi} \int_0^\infty \rho(u)^{-1} \cos \theta(u) du$$

706   A FORTRAN implementation of these numerical integrations is given by Farebrother (1990).

     Patnaik Approximation. An alternative quick way of computing an approximation to equation (11) is to see that a mixture of χ_1^2 can be approximated by $c\chi_\nu^2$ ran-
711 dom variables (Johnson *et al.*, 1995; Patnaik, 1949) for $c = \sum_{k=1}^q l_k^2 / \sum_{k=1}^q l_k$ and $\nu = (\sum_{k=1}^q l_k)^2 / \sum_{k=1}^q l_k^2$. Generally, since $q \leq 2$, it follows that if $l_1 >> l_2$, then $c \approx l_1$ and $\nu \approx 1$, whereas if $l_1 \approx l_2$, then $c \approx l_1$ and $\nu \approx 2$. Note that this approximation entails the use of a χ^2 distribution with non-integer ν which can be computed using the gamma function
716 (Johnson *et al.*, 1995).

721

726

731

736

741

746